

In Situ Quantitative Graphene-Based Surface-Enhanced Raman Spectroscopy

Huihui Tian, Na Zhang, Lianming Tong,* and Jin Zhang*

Quantitative surface-enhanced Raman spectroscopy (SERS) with ultrahigh sensitivity will significantly promote its practical application in many fields, such as environment monitoring, food safety, and drug detection. However, the challenges that remain unresolved, particularly in the low concentration levels, arise from the instability of the SERS spectra and the uncertainty of the number of detected molecules. Herein, a graphene-based, flexible, and transparent substrate for SERS quantification is reported, wherein the 2D single-crystalline nature of graphene promises the homogeneous adsorption of molecules, facilitating the determination of the number of molecules, the separation of molecules from metal, which ensures the stability of the Raman signals, and an internal standard for the calibration of SERS intensities. The in situ quantification of probe molecules is demonstrated in an aqueous solution down to the detection limit of 10^{-8} M, and the real-time, in situ monitoring of the release process of rhodamine B molecules, which mimics practical application, for example, the controlled release of medicine, is shown. The results open up an avenue for reliable SERS quantification for practical applications with high efficiency and low cost.

1. Introduction

Surface-enhanced Raman spectroscopy (SERS) has been widely used in chemo/biosensing to detect trace species.^[1–5] With optimized metal-nanostructured substrates, SERS can reach single-molecule sensitivity and can detect whether or not an analyte exists. On the other hand, the quantity of the analyte is of equivalent importance and is a must in certain fields, such as the in situ detection of contaminants for quality control and the in vivo monitoring of medicines in sustained-release. To date, several approaches have been developed aiming at reliable quantitative SERS analysis with high resolution and sensitivity, including the implement of internal standards and univariate and multivariate data analysis methods.^[6–11] However, the problems that hinder the practical application of SERS quantification include the spectral instability, the inhomogeneous electromagnetic enhancement, and

the uncertainty of the amount of detected molecules. The spectral instability is mainly due to the orientation fluctuation of molecules and/or the possible chemical reactions between the molecules and the metal substrate.^[12–14] In principle, this can be avoided by isolating the molecules from the metal surface, for example, by coating a dielectric nanoshell on the metal nanostructures.^[6,14,15] The inhomogeneous electromagnetic enhancement can be largely calibrated by implementing an internal standard species that experiences the same enhancement as the analyte molecule, so that the ratio between the Raman intensities of the analyte and the internal standard can be used for quantification.^[6,16,17] The uncertainty of the amount of detected molecules is the most notorious because there have been few solutions so far, and the rough estimation of the number of molecules based on the homogenous-adsorption assumption

and the detection area/volume has been generally adopted, although the probability of molecules adsorption is different on different facets of the metal nanostructures.

Herein, we report a graphene-based SERS (G-SERS) substrate for analyte quantification that solves the above problems to a great extent. Graphene has shown its unique characteristics in SERS applications.^[18–21] For example, graphene quenches the fluorescence of fluorophores and provides stable and clean Raman signals due to the separation of molecules from a metal.^[18,19] Graphene has also been used to cover the surface of plasmonic nanostructures and the composite substrate can provide remarkable Raman enhancement.^[22,23] More importantly, the single-crystalline nature of graphene guarantees that the probe molecules are homogeneously adsorbed on the surface, rendering the possibility of reliable determination of the number of molecules. Meanwhile, graphene is naturally an internal standard for the normalization of the Raman signals of analytes, so that the different enhancement experienced by molecules at different locations can be calibrated. In our substrate, a roughened metal film under graphene ensures that the overall Raman enhancement is still dominated by the sizable electromagnetic enhancement. We demonstrated in situ quantitative detection of crystal violet (CV) and rhodamine B (RhB) molecules in aqueous solutions with concentrations from 10^{-8} to 10^{-5} M and the real-time monitoring of a release process of RhB molecules through a permeable membrane. Our graphene-based SERS substrate promises SERS quantification

Dr. H. Tian, N. Zhang, Prof. L. Tong, Prof. J. Zhang
Center for Nanochemistry
State Key Laboratory for Structural Chemistry of Unstable
and Stable Species
College of Chemistry and Molecular Engineering
Peking University
Beijing 100871, China
E-mail: tonglm@pku.edu.cn; jinzhang@pku.edu.cn

DOI: 10.1002/smt.201700126

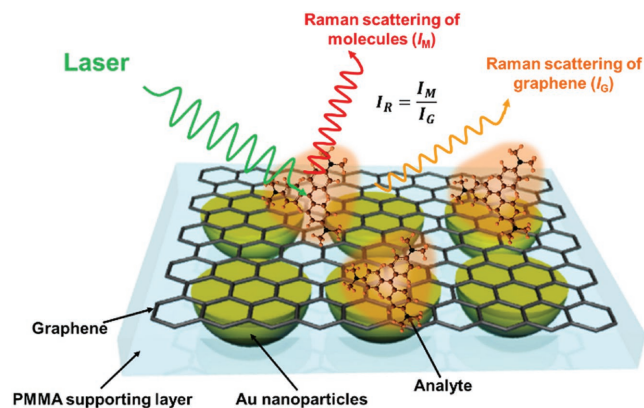


Figure 1. Scheme of quantitative analysis using graphene-based surface-enhanced Raman scattering (G-SERS).

in a variety of areas including environmental, toxicological, and biomedical applications.

2. Results

Figure 1 illustrates the scheme of the graphene-based substrate for SERS quantification. Such a substrate can float on aqueous solution for in situ SERS sensing. The experimental details on the fabrication and characterization can be found in the Supporting Information (Figure S1). During the SERS measurement, the Raman scattered signals from the molecules (I_M) and graphene (I_G) are simultaneously collected. By using I_G as

an internal standard, the variation of I_M over the whole surface due to the random distribution of electromagnetic hotspots and the instrumental/measurement drift can be calibrated and the relative intensity I_R is then obtained for further analysis.

The homogeneous adsorption of organic molecules on graphene has been investigated by scanning tunneling microscopy studies and theoretical calculations,^[24–29] and thus, for analyte molecules in an aqueous solution, the adsorption probability on the G-SERS substrate is also expected to be homogeneous at the sub-monolayer level. In an aqueous solution, dye molecules are usually positively charged. The electrostatic interaction also ensures a monolayer adsorption without aggregations. The coverage of molecules on graphene can be obtained according to the Langmuir isothermal model (see below), which can be correlated to the calibrated signal I_R .

Figure 2 demonstrates the Raman intensity homogeneity of CV molecules adsorbed on a single-layer graphene transferred onto an SiO_2/Si substrate with poly(dimethylsiloxane) (PDMS) (see “Transfer of graphene onto SiO_2/Si with PDMS” in the Supporting Information for experimental details).^[30] The concentration of CV solution was 10^{-6} M. Figure 2a,b shows the optical and Raman mapping images of CV at 1180 cm^{-1} from 100 Raman spectra (overlaid in Figure 2c), respectively. The relative standard deviation (RSD) of the peak intensity is 10%. At the same time, the RSD of the 2D peak at 2650 cm^{-1} of graphene is 6%, which implies the good quality of graphene. The uniform distribution of the Raman signal indicates that the CV molecules were indeed distributed homogeneously on the graphene surface (also see Figure S2, Supporting Information). It is worth noting that the most direct evidence would be in

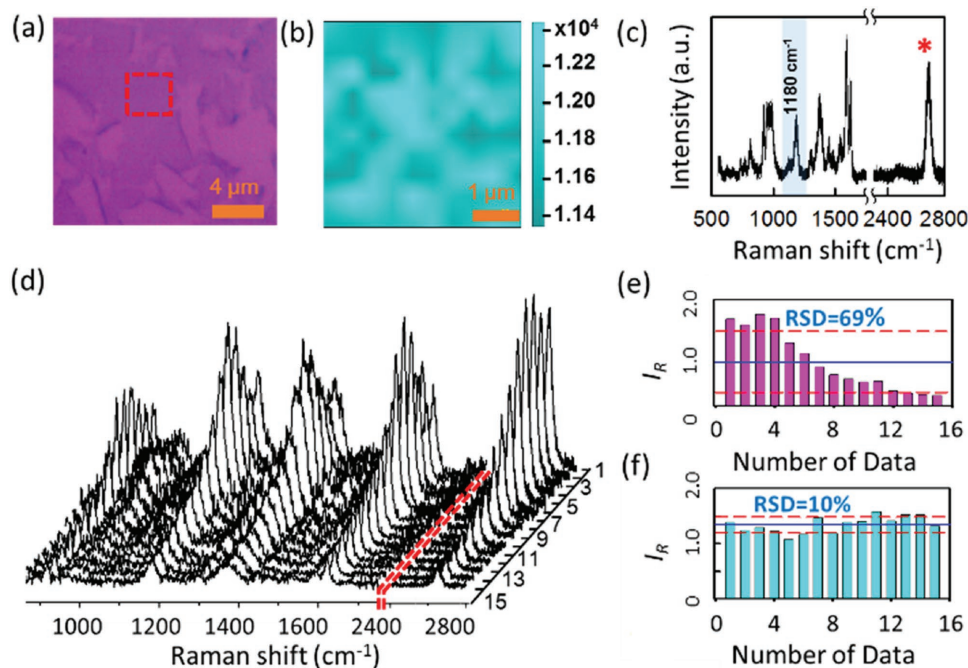


Figure 2. a) Optical image of monolayer graphene transferred on SiO_2/Si substrate. b) Raman mapping image of crystal violet (CV) at 1180 cm^{-1} in the squared area shown in (a). c) The corresponding overlaid Raman spectra for mapping in (b). d) A series of Raman spectra of CV at different locations on a G-SERS substrate with different laser focus status. e,f) The statistics of the peak intensities at 1180 cm^{-1} of CV (e), showing a large relative standard deviation of 69%, and of the intensity ratio I_R using the 2D peak of graphene as internal standard (f), showing a significantly reduced RSD of 10%.

situ morphological measurements at single-molecular resolution in an aqueous solution of molecules after the adsorption is saturated. However, our Raman mapping measurements over different areas of tens of micrometers could already evidence the homogeneous adsorption of molecules, that is, there is no trend of obvious aggregation and the surface density of molecules on graphene is independent of the position and the area of measurement.

In order to demonstrate the role of the internal standard using I_G , a G-SERS substrate with metal nanoparticles was directly placed on the CV aqueous solution with a concentration of 10^{-7} M for Raman measurement. We chose the 2D peak of graphene as the internal standard because of two reasons: the 2D peak of graphene at 2650 cm^{-1} is far from the typical frequency window of commonly used dye molecules, and the intensity of the 2D peak is the strongest for monolayer graphene. Figure 2d shows the SERS spectra of CV on different locations with different laser focus statuses. It is obvious that the Raman intensities of the CV molecules and the graphene fluctuated simultaneously. However, if we normalize the peak intensity of CV (1180 cm^{-1}) to that of graphene (2650 cm^{-1}), the signal becomes much more stable. The RSD was reduced from 69% (Figure 2e) to 10% (Figure 2f), allowing reliable quantitative analysis.

Figure 3 demonstrates the results of SERS quantification using G-SERS substrate. Representative SERS spectra of CV with different concentrations are shown in Figure 3a. The SERS spectra were taken after the adsorption of the molecules on graphene was saturated (Figure S3, Supporting Information). It can be seen that the intensity of CV molecules increased with the increase of concentration, while the peak intensity of graphene also fluctuated slightly, probably due to different focus status on different samples. The limit of detection of CV using the G-SERS substrate for these measurements was 10^{-8} M (i.e., 4.1 ng mL^{-1}), as shown in Figure 3d. In order to demonstrate reliable SERS quantification, four representative peaks of CV were chosen to calibrate the intensity fluctuation and to obtain I_R (see “Selection of representative Raman peaks of CV for G-SERS quantification” of the Supporting Information for details), that is, 810 cm^{-1} (out-of-plane mode), 916 cm^{-1} (in-plane mode), 1365 cm^{-1} (in-plane mode), and 1621 cm^{-1} (in-plane mode). The results are plotted in Figure 3b for CV concentrations ranging from 10^{-8} to 10^{-5} M. Figure 3c shows the magnified plot in the low concentration range from 10^{-8} to 10^{-7} M, exhibiting a good linear relationship between I_R and CV concentration.

The number of detected molecules, essential for SERS quantification, can be acquired from the surface coverage of

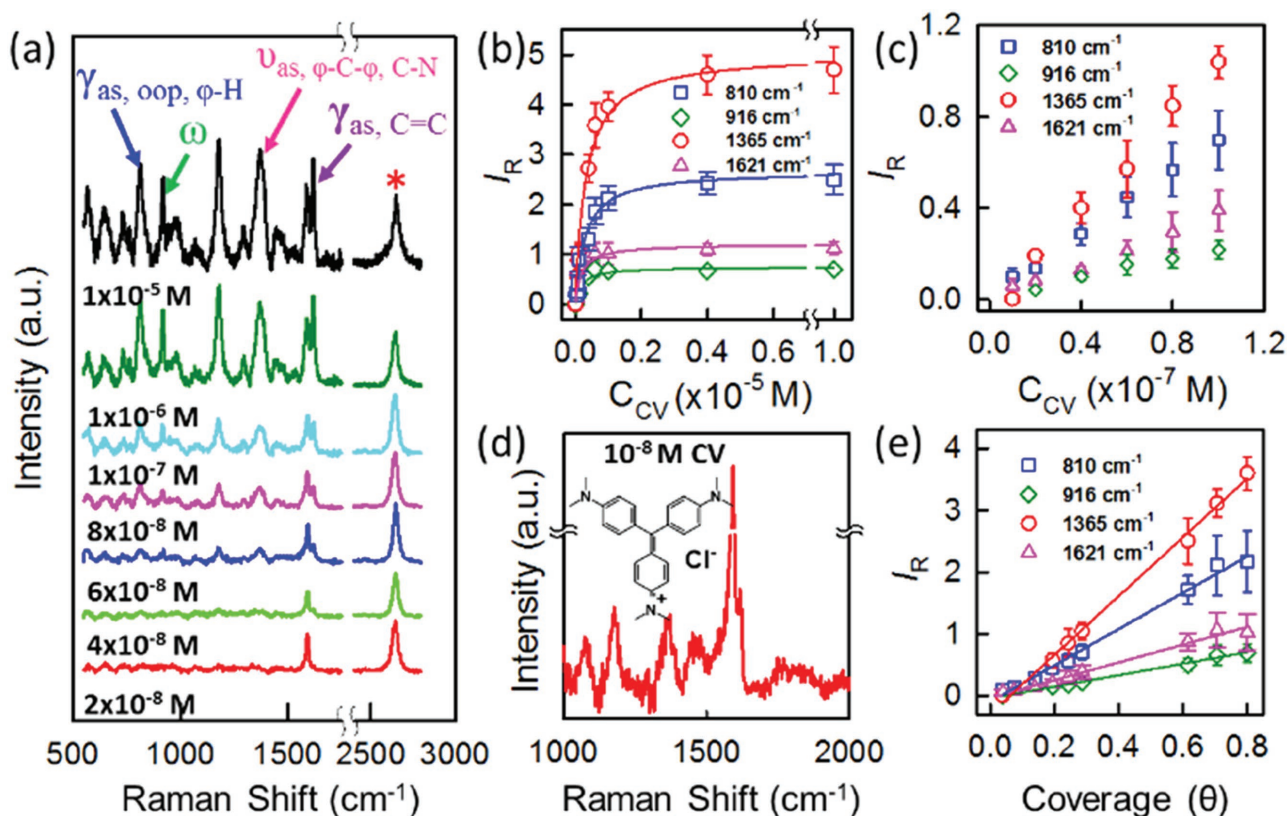


Figure 3. a) Raman spectra of crystal violet (CV) with different concentrations in the range of 10^{-8} to 10^{-5} M. b) Concentration-dependent I_R of the four peaks highlighted in (a), 810 , 916 , 1365 , and 1621 cm^{-1} , using graphene (2D peak) as internal standard. c) The magnified plots in the low concentrations from 10^{-8} to 10^{-7} M. d) The magnified spectra of CV with concentration of 10^{-8} M; the inset figure is the chemical formula of CV molecule. e) The calibrated intensities I_R as a function of surface coverage. All the spectra were obtained under 633 nm excitation. The peak marked by the asterisk (*) is the G-band of graphene.

molecules on graphene. This is attainable from the Langmuir isothermal adsorption model:^[31,32]

$$\frac{C}{I_e} = \frac{C}{I_{\max}} + \frac{1}{I_{\max} K_T} \quad (1)$$

where C is the concentration of CV molecules in solution, I_{\max} and I_e are the maximum Raman intensity in the plateau region in Figure 3b and the measured Raman intensity at concentration C at adsorption equilibrium, respectively, and K_T is the adsorption constant (L mol^{-1}) related to the binding affinity and adsorption energy of molecules on graphene. The Langmuir model assumes that the adsorption occurs on a homogeneous surface and no interaction between adsorbates in the plane of this homogeneous adsorbing surface, and the adsorption sites are independent.

Equation (1) was used to fit the data in Figure 3b, and the results are shown as the solid curves. The fitting coefficient of determination R^2 is as high as 0.998. The Langmuir constant (K_T) was obtained for the four peaks, which is $(3.35 \pm 0.25) \times 10^6 \text{ M}^{-1}$ (see “Adsorption constant of CV molecules on graphene without metal” and Figure S4 in the Supporting Information for a comparison to the adsorption of CV on graphene/SiO₂/Si substrate). The surface coverage of molecules at different concentrations can then be obtained from K_T :

$$\theta = \frac{K_T C}{1 + K_T C} \quad (2)$$

The results are plotted in Figure S5 (Supporting Information), showing a linear relationship at low concentrations from 10^{-8} to 10^{-7} M . At higher concentrations, the surface coverage became nonlinear to the concentration, indicating the near saturation of CV molecules adsorbed on the surface of graphene at high concentrations, so that the increase in concentration does not result in a linear change of the surface-coverage change as at low concentrations. It is worth pointing out that the linear relationship could not be obtained without using the Raman signal

of graphene as an internal standard (see Figure S6, Supporting Information). Besides, with the knowledge of the size of molecules and the distribution of the molecules at full coverage, the number of molecules can, in principle, be estimated under each surface coverage (see “Estimation of number of molecules on graphene” and Figure S7 in the Supporting Information).

The G-SERS substrate was then applied for the quantitative detection of RhB molecules, which is a synthetic dye with a bright rose color and used in the industries of paper and leather, but is forbidden as an additive in food production due to carcinogenic risk.^[33,34] RhB solutions with a series of concentrations in pure water were first measured (see representative G-SERS spectra in Figure S8, Supporting Information) and the working curve (I_R vs c) was plotted in Figure 4c. A nice fitting using the Langmuir isotherm model was found with $R^2 = 0.996$. The adsorption constant K_T was obtained as $(1.6 \pm 0.1) \times 10^6 \text{ M}^{-1}$. Using this working curve, one can quantify the concentration of RhB in an unknown solution with measured I_R .

To this end, an RhB aqueous solution of $1.0 \times 10^{-6} \text{ M}$ concentration was prepared. For comparison, RhB of the same concentration was also prepared by adding RhB in a soft drink (Figure 4a). The samples were then measured by using G-SERS substrates directly floating on the aqueous surface, and typical Raman spectra were shown in Figure 4b. It is apparent that for both pure RhB solution and soft drink sample, the representative peak at 1651 cm^{-1} of RhB (aromatic C–C bending and C=C stretching) are clearly seen (blue and red curves, respectively), while it disappears for the blank sample of the soft drink (black curve). The I_R values are 0.165 and 0.147, corresponding to the determined concentrations of 1.13×10^{-6} and $0.83 \times 10^{-6} \text{ M}$, respectively. The RhB concentration measured in the soft drink sample is somewhat lower by 17%. This is probably due to the competitive adsorption of other components, revealing another important challenge in SERS quantification, that is, the nonspecific adsorption of competing species in composite systems.

To further demonstrate the capability of in situ quantification in practical cases, the real-time monitoring of the release process of molecules through a membrane was tested. RhB

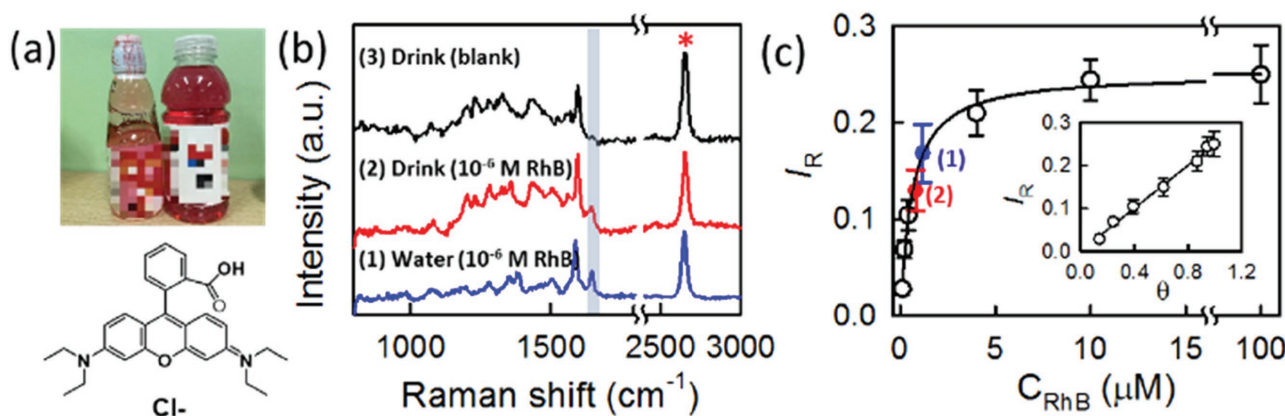


Figure 4. a) A photograph of the RhB additive (10^{-6} M) in a soft drink and the molecular structure of RhB. b) Typical Raman spectra of RhB measured using G-SERS substrate on a blank sample of the soft drink (black, curve 3), the soft drink with 10^{-6} M RhB (red, curve 2), and an aqueous solution with 10^{-6} M RhB (blue, curve 1). c) Concentration-dependent IR of RhB (1651 cm^{-1}) to 2D peak of graphene (2650 cm^{-1}). The blue and red dots are the measured data from (b), respectively. The inset shows the plot of IR versus the surface coverage of RhB on graphene. The peak marked by the asterisk (*) is the G-band of graphene.

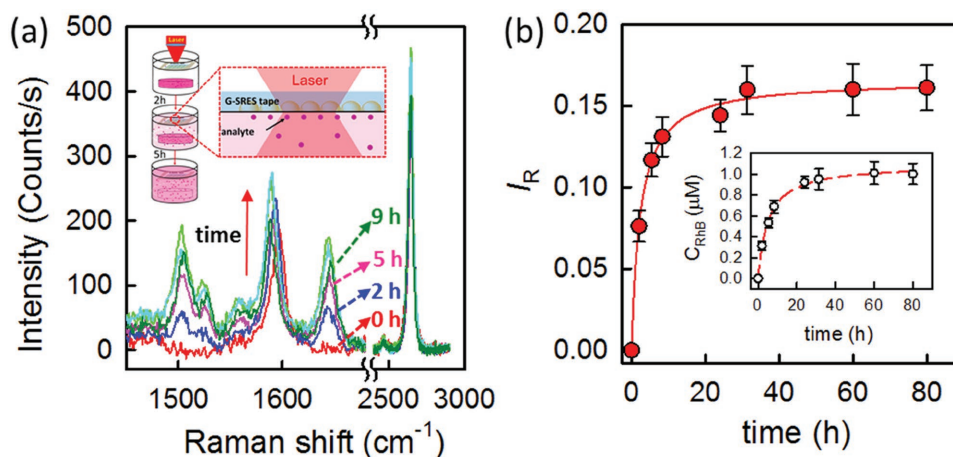


Figure 5. The real-time, in situ monitoring of RhB molecules released through a permeable membrane. The initial concentration was 1.5×10^{-5} M, and the final concentration 1.0×10^{-6} M was reached after an equilibrium time of ≈ 40 h. a) G-SERS spectra of RhB at different release time. The inset is the corresponding schematic. b) The time-dependent I_R of detected RhB. The inset shows the corresponding detected concentrations as a function of time.

molecules of initial concentration 1.5×10^{-5} M penetrating a membrane of cutoff molecular weight 500 D was used to mimic practical application, for example, in the monitoring of the controlled release of medicine (see “Real-time monitoring of molecules release through a membrane” and Figure S9 in the Supporting Information for experimental details). **Figure 5a** shows the temporal SERS spectra of detected RhB molecules using G-SERS tape, and, in **Figure 5b**, the detected I_R values as a function of time are plotted. The inset shows the corresponding detected concentrations. It is apparent that the equilibrium concentration (1.0×10^{-6} M) was reached after ≈ 40 h. From the diffusion point of view, there exists a concentration gradient between the surface of solution and the outer surface of the membrane, and the diffusion process should be described by Fick's second law. However, as the equilibrium time of molecules adsorbed on graphene (≈ 5 min) was much shorter than the interval of detection (at least 2 h), the concentration was considered homogeneous in the solution during the Raman measurement, so that the detected concentration by G-SERS tape at the surface represented the volume concentration. The analysis based on the detected concentrations shows that about 50% of the molecules were released after 5 h, and 90% were released after 31 h (Table S1, Supporting Information). For a membrane with larger pinhole size, for example, cutoff molecular weight 1000D, the release process was much faster, that is, an equilibrium time of ≈ 40 min (see Figure S10, Supporting Information). We note that such a real-time, in situ monitoring of trace species using G-SERS tape is rapid and convenient, and the detection limit, 10^{-7} to 10^{-8} M in these experiments (for CV and RhB), and the concentration range of linear signal-concentration relationship, can be further improved by optimizing the metallic nanostructures embedded in the substrate.

3. Conclusions

In summary, we have developed a graphene-based SERS substrate for quantification analysis. Graphene plays key roles in this approach: a stabilizer of Raman signals, an internal standard and

a platform for homogeneous adsorption of analyte molecules. We show the feasibility of quantification of CV molecules in aqueous with concentration ranging from 10^{-8} to 10^{-5} M. Moreover, the in situ quantification of RhB molecules in a soft drink, and the real-time, in situ monitoring of the release process of molecules that mimics the controlled release of medicine are demonstrated as examples of practical applications. Although certain challenges still remain, such as the competitive adsorption of molecules in complex systems, our approach has proven reliable SERS quantification toward practical applications.

Supporting Information

Supporting Information is available from the Wiley Online Library or from the author.

Acknowledgements

J.Z. and L.T. acknowledge funding from the NSFC (21233001, 51272006, 11374355, and 21573004) and the MOST (2016YFA0200101, 2016YFA0200104, and 2015CB932400). H.T. acknowledge funding from the China Postdoctoral Science Foundation (2016M590011). The authors thank H. Wang and B. Deng for their supply of monolayer graphene grown by the chemical vapor deposition (CVD) method for this work.

Conflict of Interest

The authors declare no conflict of interest.

Keywords

graphene, in situ, internal standards, quantitative detection, surface-enhanced Raman scattering

Received: March 1, 2017
Revised: March 31, 2017
Published online: May 16, 2017

- [1] M. Moskovits, *Rev. Mod. Phys.* **1985**, *57*, 783.
- [2] J. Popp, T. Mayerhofer, *Anal. Bioanal. Chem.* **2009**, *394*, 1717.
- [3] S. Schlücker, *Angew. Chem., Int. Ed.* **2014**, *53*, 4756.
- [4] P. Wang, O. Liang, W. Zhang, T. Schroeder, Y. H. Xie, *Adv. Mater.* **2013**, *25*, 4918.
- [5] E. C. L. Ru, P. G. Etchegoin, *Annu. Rev. Phys. Chem.* **2012**, *63*, 65.
- [6] H. Y. Chen, M. H. Lin, C. Y. Wang, Y. M. Chang, S. Gwo, *J. Am. Chem. Soc.* **2015**, *137*, 13698.
- [7] S. E. J. Bell, N. M. S. Sirimuthu, *Chem. Soc. Rev.* **2008**, *37*, 1012.
- [8] W. Shen, X. Lin, C. Jiang, C. Li, H. Lin, J. Huang, S. Wang, G. Liu, X. Yan, Q. Zhong, B. Ren, *Angew. Chem., Int. Ed.* **2015**, *54*, 7308.
- [9] E. Kämmer, K. Olschewski, S. Stöckel, P. Rösch, K. Weber, D. Cialla-May, T. Bocklitz, J. Popp, *Anal. Bioanal. Chem.* **2015**, *407*, 8925.
- [10] Y. Wang, S. Kang, A. Khan, G. Ruttner, S. Y. Leigh, M. Murray, S. Abeytunge, G. Peterson, M. Rajadhyaksha, S. Dintzis, S. Javid, J. T. C. Liu, *Sci. Rep.* **2016**, *6*, 21242.
- [11] S. Gwo, C. Y. Wang, H. Y. Chen, M. H. Lin, L. Sun, X. Li, W. L. Chen, Y. M. Chang, H. Ahn, *ACS Photonics* **2016**, *3*, 1371.
- [12] R. P. Cooney, M. R. Mahoney, M. W. Howard, *Chem. Phys. Lett.* **1980**, *76*, 448.
- [13] B. Dong, Y. Fang, X. Chen, H. Xu, M. Sun, *Langmuir* **2011**, *27*, 10677.
- [14] J. F. Li, Y. F. Huang, Y. Ding, Z. L. Yang, S. B. Li, X. S. Zhou, F. R. Fan, W. Zhang, Z. Y. Zhou, D. Y. Wu, B. Ren, Z. L. Wang, Z. Q. Tian, *Nature* **2010**, *464*, 392.
- [15] J. F. Li, J. R. Anema, T. Wandlowski, Z. Q. Tian, *Chem. Soc. Rev.* **2015**, *44*, 8399.
- [16] S. Xu, S. Jiang, J. Wang, J. Wei, W. Yue, Y. Ma, *Sens. Actuators, B* **2016**, *222*, 1175.
- [17] L. Zou, L. Chen, Z. Song, D. Ding, Y. Chen, Y. Xu, S. Wang, X. Lai, Y. Zhang, Y. Sun, Z. Chen, W. Tan, *Nano Res.* **2016**, *9*, 1418.
- [18] L. Xie, X. Ling, Y. Fang, J. Zhang, Z. Liu, *J. Am. Chem. Soc.* **2009**, *131*, 9890.
- [19] X. Ling, L. Xie, Y. Fang, H. Xu, H. Zhang, J. Kong, M. S. Dresselhaus, J. Zhang, Z. Liu, *Nano Lett.* **2010**, *10*, 553.
- [20] W. Xu, J. Xiao, Y. Chen, Y. Chen, X. Ling, J. Zhang, *Adv. Mater.* **2013**, *25*, 928.
- [21] W. Xu, X. Ling, J. Xiao, M. S. Dresselhaus, J. Kong, H. Xu, Z. Liu, J. Zhang, *Proc. Natl. Acad. Sci. USA* **2012**, *109*, 9281.
- [22] P. Wang, W. Zhang, O. Liang, M. Pantoja, J. Katzer, T. Schroeder, Y.-H. Xie, *ACS Nano* **2012**, *7*, 6244.
- [23] F. Schedin, E. Lidorikis, A. Lombardo, V. G. Kravets, A. K. Geim, A. N. Grigorenko, K. S. Novoselov, A. C. Ferrari, *ACS Nano* **2010**, *4*, 5617.
- [24] M. Roos, D. Künzel, B. Uhl, H. H. Huang, O. B. Alves, H. E. Hoster, A. Gross, J. R. Behm, *J. Am. Chem. Soc.* **2011**, *133*, 9208.
- [25] N. Batina, M. Kunitake, K. Itaya, *J. Electroanal. Chem.* **1996**, *405*, 245.
- [26] P. Lazar, F. Karlický, P. Jurečka, M. Kocman, E. Otyepková, K. Šafářová, M. Otyepka, *J. Am. Chem. Soc.* **2013**, *135*, 6372.
- [27] L. Kong, A. Enders, T. S. Rahman, P. A. Dowben, *J. Phys.: Condens. Matter* **2014**, *26*, 443001.
- [28] Y. Su, H.-L. Han, Q. Cai, Q. Wu, M. Xie, D. Chen, B. Geng, Y. Zhang, F. Wang, Y. R. Shen, C. Tian, *Nano Lett.* **2015**, *15*, 6501.
- [29] Q. H. Wang, M. C. Hersam, *Nat. Chem.* **2009**, *1*, 206.
- [30] X. Li, W. Cai, J. An, S. Kim, J. Nah, D. Yang, R. Piner, A. Velamakanni, I. Jung, E. Tutuc, S. K. Banerjee, L. Colombo, R. S. Ruoff, *Science* **2009**, *324*, 1312.
- [31] I. Langmuir, *J. Am. Chem. Soc.* **1918**, *40*, 1361.
- [32] T. Liu, Y. Li, Q. Du, J. Sun, Y. Jiao, G. Yang, Z. Wang, Y. Xia, W. Zhang, K. Wang, H. Zhu, D. Wu, *Colloids Surf., B* **2012**, *90*, 197.
- [33] R. Jain, M. Mathur, S. Sikarwar, A. Mittal, *J. Environ. Manage.* **2007**, *85*, 956.
- [34] P. Qi, Z. Lin, J. Li, C. L. Wang, W. W. Meng, H. Hong, X. W. Zhang, *Food. Chem.* **2014**, *164*, 98.